Chemical Science

ROYAL SOCIETY OF CHEMISTRY

EDGE ARTICLE

View Article Online
View Journal | View Issue



Cite this: *Chem. Sci.*, 2023, **14**, 5369

All publication charges for this article have been paid for by the Royal Society of Chemistry



# Unconventional gas-phase preparation of the prototype polycyclic aromatic hydrocarbon naphthalene ($C_{10}H_8$) *via* the reaction of benzyl ($C_7H_7$) and propargyl ($C_3H_3$) radicals coupled with hydrogen-atom assisted isomerization†

Chao He, [a] Ralf I. Kaiser, *[a] Wenchao Lu, [b] Musahid Ahmed, *[b] Vladislav S. Krasnoukhov,[cd] Pavel S. Pivovarov,[d] Marsel V. Zagidullin,[c] Valeriy N. Azyazov, [c] Alexander N. Morozov[e] and Alexander M. Mebel *[e]

Polycyclic aromatic hydrocarbons (PAHs) are ubiquitous in the interstellar medium and in meteorites such as Murchison and Allende and signify the missing link between resonantly stabilized free radicals and carbonaceous nanoparticles (soot particles, interstellar grains). However, the predicted lifetime of interstellar PAHs of some $10^8$ years imply that PAHs should not exist in extraterrestrial environments suggesting that key mechanisms of their formation are elusive. Exploiting a microchemical reactor and coupling these data with computational fluid dynamics (CFD) simulations and kinetic modeling, we reveal through an isomer selective product detection that the reaction of the resonantly stabilized benzyl ($C_7H_7^{\bullet}$) and the propargyl ($C_3H_3^{\bullet}$) radicals synthesizes the simplest representative of PAHs – the 10π Hückel aromatic naphthalene ($C_{10}H_8$) molecule – *via* the novel Propargyl Addition–BenzAnnulation (PABA) mechanism. The gas-phase preparation of naphthalene affords a versatile concept of the reaction of combustion and astronomically abundant propargyl radicals with aromatic radicals carrying the radical center at the methylene moiety (aromatic-$CH_2^{\bullet}$) as a previously passed over source of aromatics in high temperature environments thus bringing us closer to an understanding of the aromatic universe we live in.

Received 17th February 2023
Accepted 19th April 2023

DOI: 10.1039/d3sc00911d

rsc.li/chemical-science

## Introduction

Since the pioneering observation of the simplest organic radical methylidyne (CH) toward ζ-Oph by Swings and Rosenfeld in 1973,[1] resonantly stabilized free radicals–organic radicals in which the unpaired electron is delocalized over multiple carbon atoms – such as propargyl ($C_3H_3^{\bullet}$) have been suggested as fundamental building blocks in molecular mass growth processes to polycyclic aromatic hydrocarbons (PAHs).[2–12] Polycyclic aromatic hydrocarbons (PAHs) are organic molecules consisting of fused benzene rings with naphthalene ($C_{10}H_8$) being the simplest representative.[13] Along with their protonated, ionized, (de)hydrogenated, alkylated, and nitrogen-substituted counterparts like (iso)quinoline ($C_9H_7N$), aromatics in deep space have been projected to account for up to 30% of the galactic carbon budget.[14–20] PAHs identified in carbonaceous chondrites like Allende, Murchison, and Orgueil as well as in cold molecular clouds such as the Taurus Molecular Cloud (TMC-1) through their cyano derivatives such as 1- and 2-cyanonaphthalene ($C_{10}H_7CN$)[21] may signify the missing link between resonantly stabilized free radicals and carbonaceous nanoparticles, commonly referred to as interstellar grains.[16–20,22]

Whereas on present-day Earth, PAHs along with carbonaceous nanoparticles (soot) as their descendants exemplify unwanted, often carcinogenic by-products of incomplete

[a]*Department of Chemistry, University of Hawai'i at Mānoa, Honolulu, HI 96822, USA. E-mail: ralfk@hawaii.edu*

[b]*Chemical Sciences Division, Lawrence Berkeley National Laboratory, Berkeley, CA 94720, USA. E-mail: mahmed@lbl.gov*

[c]*Lebedev Physical Institute, Samara 443011, Russian Federation*

[d]*Samara National Research University, Samara 443086, Russian Federation*

[e]*Department of Chemistry and Biochemistry, Florida International University, Miami, Florida 33199, USA. E-mail: mebela@fiu.edu*

† Electronic supplementary information (ESI) available: Experimental and computational methods, PIE curve for the species ($m/z$ = 130) in the benzyl ($C_7H_7^{\bullet}$) + propargyl ($C_3H_3^{\bullet}$) system (Fig. S1), computed ionization Franck–Condon factors and integrated PIE curves for three isomers of $C_{10}H_8$ (Fig. S2) and for two isomers of $C_{10}H_{10}$ (Fig. S3), calculated total and individual product channel rate constants for the benzyl–propargyl radical–radical reaction (Fig. S4 and S5), and optimized Cartesian coordinates (Å) and vibrational frequencies ($cm^{-1}$) for all intermediates, transition states, reactants and products involved in the reaction of benzyl + propargyl system in the format of an input file for RRKM–ME calculations employing the MESS package (Table S1). See DOI: https://doi.org/10.1039/d3sc00911d

combustion processes,[23–25] carbon-rich circumstellar environments of Asymptotic Giant Branch (AGB) stars and of planetary nebulae have been inferred as natural 'breeding grounds' of PAHs on the macroscopic scale.[26–28] However, as of now, there is still a critical lack of a fundamental understanding of the reaction pathways of polycyclic aromatics in carbon-rich interstellar envelopes. This deficiency is evident considering the predicted lifetimes of interstellar PAHs of a few $10^8$ years limited through their destruction by shock waves and galactic cosmic rays,[16,29–32] while the time scale for the injection of new PAHs from circumstellar envelopes to the interstellar medium exceeds some $10^9$ years.[32] This controversy suggests PAHs should not exist in extraterrestrial environments and in meteorites, thus implying that our knowledge on the underlying formation mechanisms to even the simplest representatives of PAHs – the 10π Hückel aromatic naphthalene ($C_{10}H_8$) molecule – in carbon rich circumstellar envelopes is still in its infancy.

Hansen and coworkers investigated molecular-growth pathways in propyne-doped low-pressure premixed flames of benzene and toluene and suggested that benzyl ($C_7H_7^\bullet$) radicals contribute to naphthalene formation through reactions with propargyl ($C_3H_3^\bullet$) radical along with the involvement of phenyl-substituted butadienyl and vinylacetylene isomers.[33] The kinetics and mechanisms of the recombination reaction between benzyl ($C_7H_7^\bullet$) and propargyl ($C_3H_3^\bullet$) radicals have been theoretically studied by utilizing the B3LYP, CBS-QB3, and CASPT2 quantum chemical methods, as well as the steady-state unimolecular master equation analysis based on the Rice–Ramsperger–Kassel–Marcus theory.[34] Here, we report on the results of molecular beams experiments combined with electronic structure calculations along with computational fluid dynamics (CFD) and kinetic modeling of the reaction between the resonantly stabilized benzyl ($C_7H_7^\bullet$) and the propargyl ($C_3H_3^\bullet$) radicals. The experiments exploit a chemical microreactor coupled with isomer-specific detection of the naphthalene molecule ($C_{10}H_8$) as the prototype PAH carrying two fused benzene rings through tunable vacuum ultraviolet (VUV) light. The barrierless additions of the aromatic and resonantly stabilized benzyl radical ($C_7H_7^\bullet$) to the methylenic ($CH_2$) or acetylenic (CH) moieties of the resonantly stabilized propargyl ($C_3H_3^\bullet$) radical access the 3-butynylbenzene or 2,3-butadienylbenzene ($C_{10}H_{10}$) collision complexes, which undergo facile isomerization (hydrogen migration, ring closure) followed by atomic hydrogen loss to distinct methylene-indanyl radicals ($C_{10}H_9^\bullet$). At elevated temperatures, these radicals undergo yet another hydrogen atom loss accessing benzofulvene ($C_{10}H_8$) and naphthalene ($C_{10}H_8$). This facile Propargyl Addition–BenzAnnulation (PABA) mechanism involving the reaction of astronomically abundant propargyl radicals[35] with aromatic radicals carrying the radical center at the off-ring methylene moiety (aromatic-$CH_2^\bullet$) with benzyl ($C_7H_7^\bullet$) to naphthalene and perhaps higher order PAHs like anthracene and phenanthrene signifies a fundamental shift in the perception that PAHs are predominantly formed *via* the Hydrogen-Abstraction–Acetylene Addition (HACA) pathway in carbon rich circumstellar envelopes.[13]

# Results

## Mass spectra

The reaction between the resonantly stabilized benzyl ($C_7H_7^\bullet$) and propargyl ($C_3H_3^\bullet$) radicals was explored by exploiting a chemical micro reactor[36] with radicals prepared *in situ* through flash pyrolysis of the benzylbromide ($C_6H_5CH_2Br$)[37] and propargyl bromide ($C_3H_3Br$)[38] precursors, respectively, within a heated silicon carbide tube at 1473 K. The products were entrained in a molecular beam, ionized *via* fragment-free, soft photoionization[39] using tunable synchrotron vacuum ultraviolet (VUV) light, and detected isomer-specifically with a reflectron time-of-flight mass spectrometer (Re-TOF-MS) by scanning the photon energy from 7.90 to 10.05 eV (ESI†). A representative mass spectrum recorded at a photon energy of 9.50 eV for the reaction of the benzyl with propargyl radicals at a reactor temperature of 1473 K is shown in Fig. 1. Control experiments of helium-seeded benzylbromide and propargyl bromide precursors within the identical experimental setup were also studied by keeping the silicon carbide tube at 298 K (Fig. 1a). We would like to highlight that the self-recombination of propargyl[38] or of benzyl radicals[37] does not lead to signal from $m/z = 128$ to 130. Hence, a comparison of the mass spectra provides compelling evidence that signal at $m/z =$

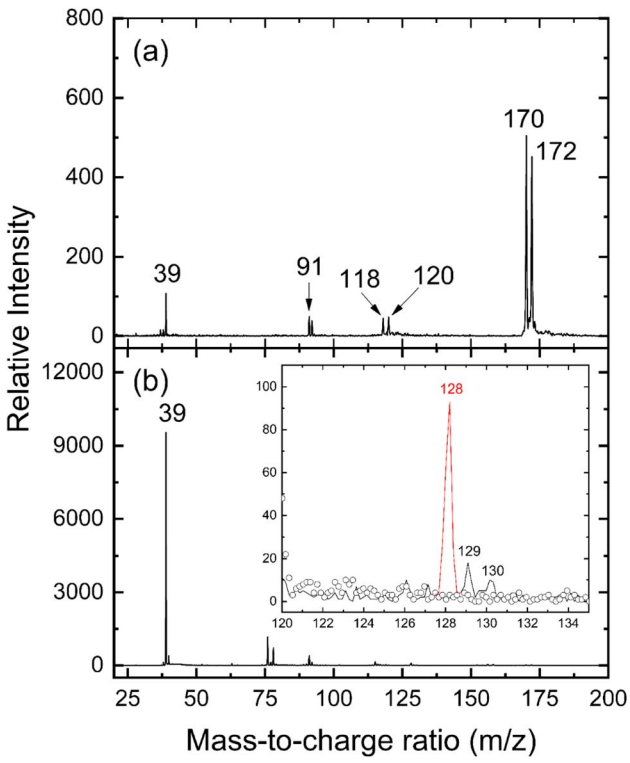


Fig. 1 Photoionization mass spectra recorded at a photon energy of 9.50 eV for the benzyl ($C_7H_7^\bullet$; $m/z = 91$) plus propargyl ($C_3H_3^\bullet$; $m/z = 39$) reaction at a temperature of 298 K (a) and 1473 ± 10 K (b). At 298 K, $m/z = 118$ and 120 are $C_3H_3{}^{79}Br$ and $C_3H_3{}^{81}Br$, and $m/z = 170$ and 172 are $C_6H_5CH_2{}^{79}Br$ and $C_6H_5CH_2{}^{81}Br$, respectively, whereas the small portion of propargyl and benzyl radicals are generated *via* dissociative photoionization. The inset in (b) highlights ion signal from $m/z = 120$ to 135 including naphthalene and potential isomers ($C_{10}H_8$; $m/z = 128$) at 298 K (open circles) and 1473 ± 10 K (solid line), respectively.

128 ($C_{10}H_8^+$), 129 ($^{13}CC_9H_8^+$ and $C_{10}H_9^+$), and 130 ($C_{10}H_{10}^+$) is linked to the reaction of benzyl with propargyl radicals (Fig. 1b); signal at these $m/z$ ratios is absent in the control experiment (Fig. 1a). Note that the intensity of the ion counts at $m/z = 128$ ($C_{10}H_8^+$) increases, whereas those at $m/z = 129$ and 130 diminish as the temperature of the reactor increases from 1173 K to 1473 K (Fig. 2). Due to the natural abundance of $^{13}C$, the $^{13}CC_9H_8^+$ should only contribute up to 11% to the total intensity of $m/z = 129$, which suggests that there should be a significant amount of $C_{10}H_9^+$. Accounting for the molecular weight of the reactants ($C_7H_7^\bullet$, 91 amu; $C_3H_3^\bullet$, 39 amu) and products ($C_{10}H_8$, 128 amu; $C_{10}H_{10}$, 130 amu), species with the molecular formula $C_{10}H_{10}$ can be linked to reaction products of the benzyl–propargyl radical–radical recombination. The temperature-dependance study (Fig. 2b) reveals that the higher temperature favors hydrogen loss and thus gradually consumes the signal of $C_{10}H_{10}^+$ to $C_{10}H_9^+$ and $C_{10}H_8^+$. At our highest experimental temperature of 1473 K, the ion counts of $m/z = 129$ stabilize at a level of $(13 \pm 4)\%$ to $m/z = 128$, whereas $m/z = 130$ is almost depleted, indicating that there remains mostly $^{13}CC_9H_8^+$ in $m/z = 129$. To summarize, the analysis of the mass spectra alone reveals that the reaction of the benzyl ($C_7H_7^\bullet$) with the propargyl ($C_3H_3^\bullet$) radical synthesizes hydrocarbon molecules with the molecular formulae $C_{10}H_{10}$ and $C_{10}H_8$ in the gas-phase.

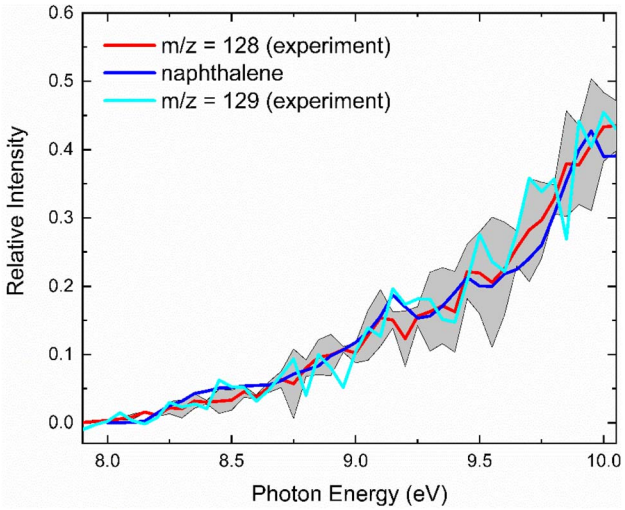


Fig. 3 Experimental PIE curves of mass-to-charge ratios of $m/z = 128$ (red) and $m/z = 129$ (cyan) recorded in the reaction of the benzyl radical with propargyl radicals at a reactor temperature of $1473 \pm 10$ K. The reference PIE curve of naphthalene is shown in blue. The error bars consist of two parts: ±10% based on the accuracy of the photodiode and a $1\sigma$ error of the PIE curve averaged over the individual scans.

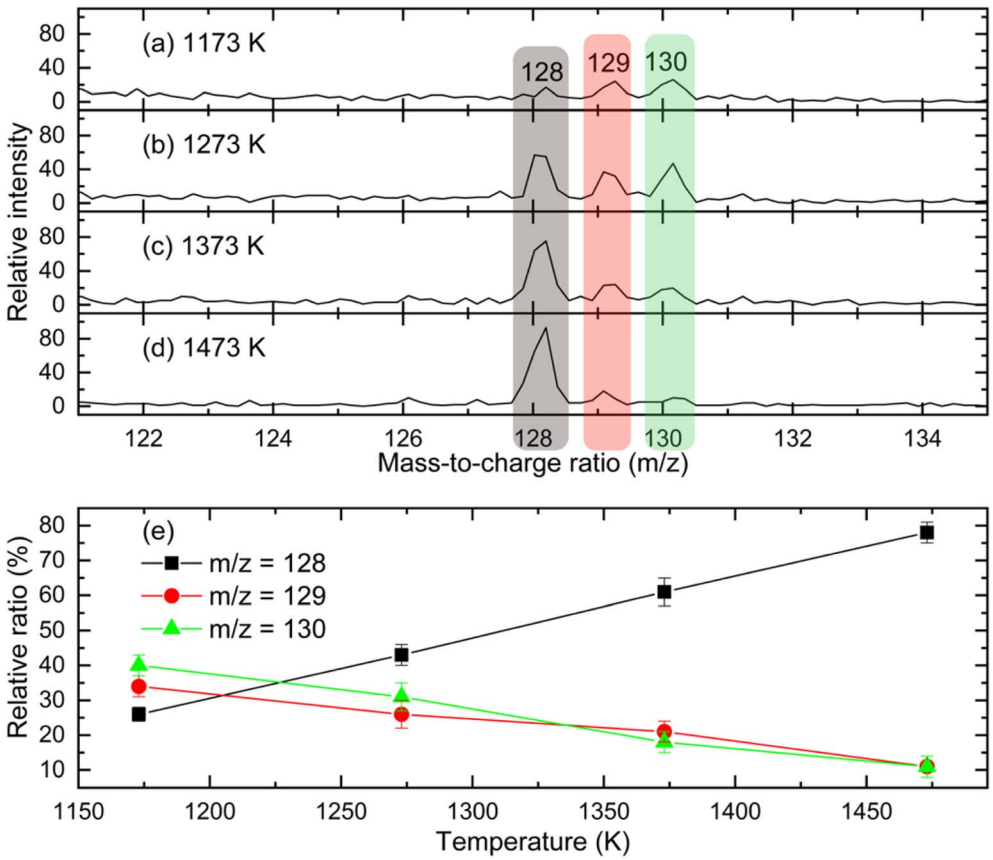


Fig. 2 Photoionization mass spectra from $m/z = 121$ to 135 recorded at a temperature of 1173 K (a), 1273 (b), 1373 (c), and 1473 K (d) at a photon energy of 9.50 eV for the benzyl ($C_7H_7^\bullet$) plus propargyl ($C_3H_3^\bullet$) reaction along with the relative ratio of $m/z = 128$, 129, and 130 as a function of the micro reactor temperature (e).

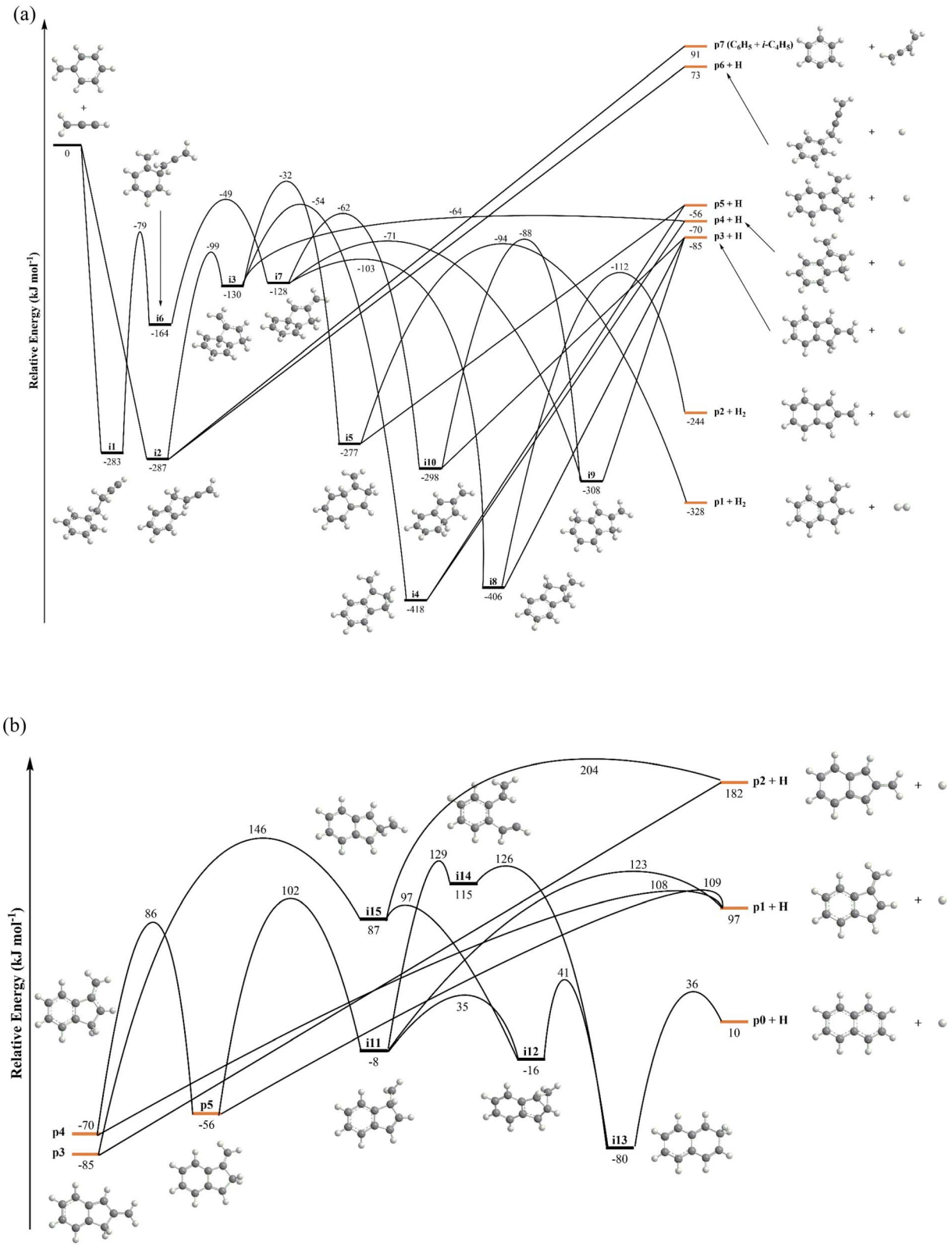


Fig. 4 (a) Main reaction pathways for the benzyl ($C_7H_7^{\bullet}$) plus propargyl ($C_3H_3^{\bullet}$) reaction. All energies are given in kJ mol$^{-1}$ with respect to the energy of the separated reactants. (b) Main reaction pathways for unimolecular decomposition methylene-indanyl radicals $C_{10}H_9$ (**p3–p5**). All energies are given in kJ mol$^{-1}$ with respect to the energy of the initial reactants of the benzyl–propargyl radical–radical reaction. Atoms are colored in black (carbon) and gray (hydrogen).

### Photoionization efficiency curves

With the detection of hydrocarbon molecules of the molecular formula $C_{10}H_{10}$ and $C_{10}H_8$, it is our objective to elucidate the nature of the structural isomer(s) formed in the reaction of the benzyl with the propargyl radicals. A detailed analysis of the corresponding photoionization efficiency (PIE) curves for ions from $m/z = 128$ ($C_{10}H_8^+$) to 130 ($C_{10}H_{10}^+$) allows an elucidation of the structural isomers formed in the reaction. This PIE curve reports the intensity of a well-defined $m/z$ ratio as a function of the photon energy from 7.90 to 10.0 eV (Fig. 3). The experimentally derived PIE curve at $m/z = 128$ (red) can be reproduced effectively by the reference PIE curve of naphthalene ($C_{10}H_8$, blue) at the highest temperature of 1473 K.[40] The PIE curves of $m/z = 129$ (cyan) and $m/z = 128$ (red) are superimposable after scaling suggesting that ions at $m/z = 129$ at 1473 K are associated with $^{13}$C-naphthalene ($^{13}CC_9H_8^+$), being congruent with our discussion about the composition of $m/z = 129$ above. Hence, we conclude that within our error limits, naphthalene ($C_{10}H_8$) denotes the only contribution to signal at $m/z = 128$. An elucidation of the structural isomers at $m/z = 130$ (Fig. S1†) is tricky since no experimental PIE curves exist for any $C_{10}H_{10}$ isomer. Therefore, these are provided *via* electronic structure calculations (ESI; Fig. S2 and S3†). However, the evaluated adiabatic IE of 1,2-dihydronaphthalene has been reported as 8.0 eV,[41] which does not match the onset of the experimental PIE curve at $m/z = 130$ at 8.95 ± 0.05 eV. Hence, 1,2-dihydronaphthalene is not formed in the reaction. Altogether, the analysis of the PIE curves at $m/z = 128$ and 130 reveals the formation of naphthalene and possibly to a minor extent benzofulvene ($C_{10}H_8$; 128 amu) as well as 3-butynylbenzene ($HCCCH_2CH_2C_6H_5$; $C_{10}H_{10}$; 130 amu).

### Reaction mechanisms – formation of methyleneindanyl radicals

The $C_{10}H_{10}$ potential energy surface (PES) accessed by the benzyl–propargyl radical reaction has been described in detail in previous publications;[34,42] here we focus on the channels which are relevant to the experimental conditions of the present study and to conditions in high temperature circumstellar envelopes (Fig. 4a, b, 5, S2–S5 and Table S1†). The resonance stabilized propargyl radical ($C_3H_3^\bullet$) can recombine barrierlessly with its radical center located at the methylenic ($CH_2$) or acetylenic (CH) moiety with the benzyl radical ($C_7H_7^\bullet$) (Fig. 4a) forming intermediates **i1** (3-butynylbenzene, $C_{10}H_{10}$) and **i2** (2,3-butadienylbenzene, $C_{10}H_{10}$), respectively; these are stabilized by 283 and 287 kJ mol$^{-1}$ with respect to the separated reactants. The subsequent reaction mechanism features a closure of the five-membered ring involving the newly added $C_3H_3$ moiety producing various methylene-indane isomers (**i3–i5**; **i7–i9**), followed by hydrogen atom migrations conserving the same methylene-indane skeleton, and completed by an atomic hydrogen loss leading to isomers of the methylene-indanyl radical (**p3–p5**). In particular, **i2** undergoes ring closure to 1-methylene-indane **i3**; the latter can eliminate atomic hydrogen forming the 1-methylene-2-indanyl **p4** product *via* a low exit barrier of only 6 kJ mol$^{-1}$ above the products with the overall

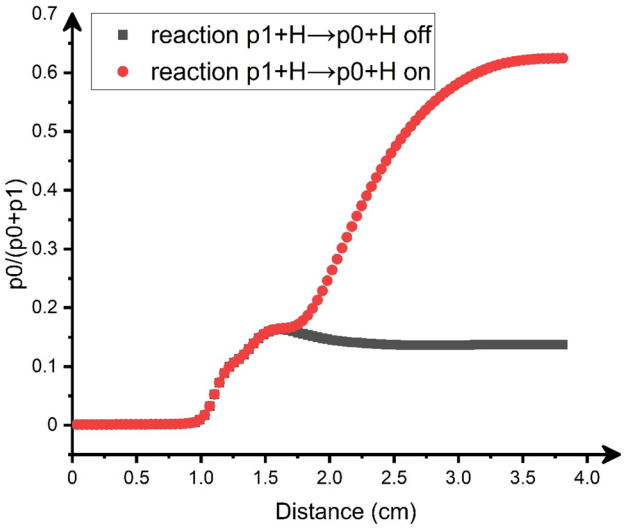


Fig. 5 Relative yield of naphthalene (**p0**) with respect to the total yield of $C_{10}H_8$ calculated with computational fluid dynamics (CFD) and kinetic simulations with and without hydrogen atom assisted isomerization of benzofulvene (**p1**) to naphthalene (**p0**). The *x*-axis specifies the distance along the length of the micro reactor.

reaction exoergicity of 70 kJ mol$^{-1}$. Alternatively, hydrogen atom shifts in **i3** can lead to **i4** or **i5** *via* barriers which are higher than that for the hydrogen atom loss. In turn, **i4** can decompose without exit barriers to **p4** and also to 3-methylene-1-indanyl **p5**. The **i5** intermediate can dissociate *via* hydrogen atom loss to **p5** without an exit barrier and may also eliminate a molecular hydrogen producing benzofulvene (1-methylene-1*H*-indene) **p1** *via* a tight exit transition state. Although these products are thermodynamically favored compared to the hydrogen atom loss products **p4**/**p5**, the molecular hydrogen loss is not competitive with the atomic hydrogen loss pathways according to the kinetics calculations (Fig. S4†). The five-membered ring closure in the initial complex **i1** has to be preceded by a shift of the $C_3H_3$ moiety to the *ortho* carbon atom in the ring, **i1** → **i6**; in principle, **i6** can be also accessed by the addition of propargyl by its CH end to the *ortho* carbon of benzyl. Next, the five-membered ring closure in **i6** results in 2-methylene-indane **i7**. A facile 1,2-H migration in **i7** from the edge connecting the six- and five-membered rings to the neighboring CH group in the five-membered ring requires a barrier of only 25 kJ mol$^{-1}$ and produces a low-lying $C_{2v}$ symmetric isomer **i8**. The latter can eliminate one of four symmetric hydrogen atoms from $CH_2$ groups in the five-membered ring forming 2-methylene-1-indanyl **p3** without an exit barrier; alternatively, a molecular hydrogen loss leading to 2-benzofulvene (2-methylene-2*H*-indene) **p2** *via* a tight transition state and high transition state was computed; again, this channel is not competitive with the hydrogen atom loss. Two other hydrogen atom shifts in **i7** can lead to **i9** and **i10**, but they feature higher barriers as compared to the one for **i7** → **i8**. The **i9** and **i10** isomers are also connected *via* a hydrogen atom migration; both of them can split a hydrogen atom forming **p3** without exit barriers. In summary, the most favorable exit channels of the benzyl–propargyl reaction

include **i2** → **p4** + H and **i1** → **i6** → **i7** → **i8** → **p3** + H *via* **i2** and **i1**, respectively. These lead to the formation of methylene-indanyl radicals, which are precursors of benzofulvene and naphthalene as discussed in the following paragraph.

The total and individual product channel reaction rate constants computed at the pressure of 30 torr representative of the hot reactive zone in the micro reactor are illustrated in Fig. S4a.†[36,43] At lower temperatures, the radical recombination is followed by collisional stabilization of **i1** and **i2**, which is preferable up to 1500 K. According to the computed rate constants for the unimolecular decomposition of these two $C_{10}H_{10}$ isomers, their lifetime in the 1375–1500 K range is on the order of 2–19 μs, and the prevailing decomposition channels lead back to the reactants. Since the computed adiabatic ionization energy (IE) of 3-butynylbenzene **i1**, of 8.8 ± 0.1 eV, reveals a good match with the experimental onset of the PIE curve of $m/z = 130$ of close to 8.9 eV (Fig. S1†), a sufficient fraction of **i1** survives long enough to exit the micro reactor. On the other hand, 2,3-butadienylbenzene **i2** has a much lower computed IE of 8.4 ± 0.1 eV. The computational method employed here for the determination of the IEs typically underestimates the experiment by about 0.1 eV, *e.g.* the computed values for phenylacetylene and naphthalene are 8.68 and 8.01 eV *versus* the NIST evaluated values of 8.82 and 8.14 eV, respectively;[44] therefore, it is unlikely that **i2** contributes to the experimental PIE curve for $m/z = 130$ (Fig. S1†). The computationally predicted relative yield of **i2** is significantly lower than that of **i1** under the reactor conditions and hence, the amount of **i2** molecules that survive to exit the reactor was insufficient for their detection. At higher temperatures, the endoergic products 1-phenyl-2-butyn-4-yl ($C_6H_5CH_2CCCH_2$) plus atomic hydrogen (**p6**) and phenyl ($C_6H_5$) plus 1,3-butadien-2-yl (i-$C_4H_5$) (**p7**) take over and become dominant; but their formation does not open any pathways toward naphthalene. On the other hand, the yield of 1-methylene-2-indanyl **p4** maximizes in the 1250–1750 K temperature range, where the rate constant for its production reaches 6–7 × $10^{-14}$ $cm^3$ $molecule^{-1}$ $s^{-1}$ (Fig. S4†). In the same temperature interval, the rate constants to form alternative methylene-indanyl radicals **p3** and **p5** also reach their maximal values of about 9 × $10^{-15}$ and 3 × $10^{-15}$ $cm^3$ $molecule^{-1}$ $s^{-1}$, respectively, but they are appreciably lower than that for the formation of **p4**. It should be also noted that the rate constants to form benzofulvene isomers **p1** and **p2** along with molecular hydrogen are more than two orders of magnitude lower than that for the atomic hydrogen loss exit channel forming **p4**. While the pathway toward naphthalene plus molecular hydrogen also exists in the primary reaction, the calculated rate constant is on the order of $10^{-17}$ $cm^3$ $molecule^{-1}$ $s^{-1}$ in the relevant temperature range. Below we seek to answer, how then can the experimentally detected naphthalene isomer be formed in the microreactor?

### Reaction mechanism – reaction of methyleneindanyl radicals to benzofulvene and naphthalene

Previous calculations of the $C_{10}H_9$ PES firmly established the methylene-indanyl radicals as critical precursors of benzofulvenes (**p1**, **p2**) and naphthalene (**p0**) (Fig. 4b) at elevated temperatures.[45] Here, we briefly highlight the results by discussing the most significant reaction pathways as compiled in Fig. 4b. 1-Methylene-2-indanyl **p4** can decompose *via* atomic hydrogen loss to benzofulvene **p1** *via* a barrier of 178 kJ $mol^{-1}$ or undergoes a 1,2-H shift forming 3-methylene-1-indanyl **p5** *via* a 156 kJ $mol^{-1}$ barrier. The latter can also dissociate to **p1** *via* atomic hydrogen loss or isomerize to naphthalene (**p0**) *via* a multistep isomerization sequence involving one additional hydrogen atom migration to the *ipso* position, **i6** → **i11**, insertion of the methylene group into the C–C bond in the five-membered ring leading to the ring expansion, **i11** → **i12** → **i13**, and hydrogen atom loss from **i13** producing naphthalene **p0**. The highest barrier on the naphthalene formation pathway is 172 kJ $mol^{-1}$ relative to **p4**, which is slightly lower than that for the formation of benzofulvene. However, **p1** is produced both from **p4** and **p5** *via* relatively loose hydrogen atom loss transition states; hence, this channel is preferable from the point of view of entropy. The preference for the formation of **p1** over **p0** in unimolecular decomposition of **p4** is displayed in the rate constants for these product channels illustrated in Fig. S4c.† The RRKM–ME rate constant calculations take into account both barrier heights and entropies of activation and the multistep character of the **p4** → **p0** + H pathway as compared to the direct **p4** → **p1** + H dissociation. In particular, at 1000 and 1250 K, the computed **p4** → **p1** + H rate constant is respectively, factors of 5.9 and 4.6 higher than that for **p4** → **p0** + H. 2-Methylene-1-indanyl **p3** can dissociate only to the high-lying 2-benzofulvene **p2** plus atomic hydrogen without an exit barrier, but with a high energy demand of 267 kJ $mol^{-1}$. The alternative pathway to **p0** plus atomic hydrogen involves a hydrogen atom shift to the *ipso* position, **p3** → **i15**, followed by a facile $CH_2$ insertion into the five-membered ring, **i15** → **i12** → **i13**, and subsequent atomic hydrogen elimination.

The calculated rate constants for decomposition of the methylene-indanyl radicals (**p3**–**p5**) to benzofulvene and naphthalene are illustrated in Fig. S4c.† The rate constants are high at temperatures above 1000 K. For instance, for **p4** – the main product of the primary benzyl–propargyl radical reaction – the values at 1250 K reach 1.7 × $10^5$ and 7.7 × $10^5$ $s^{-1}$ for the **p0** plus atomic hydrogen and **p1** plus atomic hydrogen channels, respectively, corresponding to the lifetime of about 1 μs. Moreover, at higher temperatures, the calculations predict **p4** not to exist as a chemical species but to merge/equilibrate with **p0**/**p1** plus atomic hydrogen on the time scale which is faster than its collisional relaxation. Thus, at our higher experimental temperatures, **p4** is expected to rapidly dissociate to **p1** plus atomic hydrogen which is corroborated by the significant reduction in the $m/z = 129$ signal with the temperature increase (Fig. 2) accompanied with a growth of the $m/z = 128$ signal. The **p5** species decomposes faster and is less thermally stable than **p4**, whereas **p3** is more stable. The latter can survive up to 1650 K but the calculated **p3** → **p0** plus atomic hydrogen rate constant at 1500 K for its prevailing dissociation channel to naphthalene (**p0**), 3.5 × $10^5$ $s^{-1}$, corresponds to the lifetime of only about 3 μs.

### Reaction mechanism – hydrogen assisted isomerization of benzofulvene to naphthalene

In addition to the secondary decomposition of methyleneindanyl (**p3–p5**; $C_{10}H_9$), benzofulvene (**p1**) can be converted to naphthalene (**p0**) *via* a hydrogen atom assisted isomerization. The isomerization rate constant is known to be high, $4 \times 10^{-11}$ cm$^3$ molecule$^{-1}$ s$^{-1}$, in the relevant temperature range (Fig. S4d†).[45] While naphthalene (**p0**) has been clearly observed experimentally, the unequivocal identification of benzofulvene is impossible due to the unavailability of its measured PIE; this species is unstable under normal conditions. The fact that the calculated IE of benzofulvene (**p1**), 7.97 eV, is very close to that of naphthalene (**p0**), 8.01 eV, prohibits any distinction between the two isomers solely based on the onset of the experimental PIE curve. 2-Benzofulvene (**p2**) can be clearly ruled out since its calculated IE is much lower, 7.14 eV, and no ion signal is observed at this range for $m/z = 128$. To evaluate the naphthalene (**p0**)/benzofulvene (**p1**) branching ratio under the experimental conditions and to assess the role of the hydrogen assisted isomerization between them, we carried out computational fluid dynamics (CFD) and kinetic modeling of the processes in our microreactor (ESI†). According to the results (Fig. 5), at the exit of the reactor, the relative yield of naphthalene constitutes 62% of the total $C_{10}H_8$ yield. The contribution of the hydrogen-assisted isomerization is significant. When the hydrogen assisted isomerization (**p1** + H → **p0** + H) is intentionally excluded from the kinetic model, the final yield of naphthalene drops to only 14% of the total. Thus, the CFD and kinetic modeling confirms that naphthalene (**p0**) is the prevalent $C_{10}H_8$ isomer observed experimentally, but it forms mostly *via* benzofulvene (**p1**) and the contribution of the latter to the observed PIE curve at $m/z = 128$ cannot be discounted. Overall, we can conclude that the fast secondary decomposition of methylene-indanyl radicals ($C_{10}H_9$) is predicted to be responsible for the formation of benzofulvene (**p1**) and naphthalene (**p0**) *via* the following (simplified) reaction mechanism including the hydrogen assisted isomerization of benzofulvene (**p1**):

$$C_7H_7 + C_3H_3 \rightarrow C_{10}H_9\ (\mathbf{p3} + \mathbf{p4} + \mathbf{p5}) + H \quad (1)$$

$$C_{10}H_9\ (\mathbf{p3} + \mathbf{p4} + \mathbf{p5}) \rightarrow C_{10}H_8\ (\mathbf{p0}) + H \quad (2)$$

$$C_{10}H_9\ (\mathbf{p3} + \mathbf{p4} + \mathbf{p5}) \rightarrow C_{10}H_8\ (\mathbf{p1}) + H \quad (3)$$

$$C_{10}H_8\ (\mathbf{p1}) + H \rightarrow C_{10}H_8\ (\mathbf{p0}) + H \quad (4)$$

### Reaction mechanism – circumstellar envelopes and cold molecular clouds

Let us now consider the reaction kinetics under conditions of circumstellar envelopes, *i.e.*, at high temperatures and low pressures. Fig. S4b† illustrates the reaction rate constants for the benzyl–propargyl process computed in the limit of low pressure, but considering infrared radiative stabilization of the $C_{10}H_{10}$ intermediates (ESI†). One can see that in this case, stabilization of **i2** is no longer significant, whereas stabilization of **i1** prevails only up to 600 K. Above 600 K and up to 1400 K, **p4** is the main product with its rate constant being in the range of $2 \times 10^{-12}$ to $1 \times 10^{-13}$ cm$^3$ molecule$^{-1}$ s$^{-1}$, more than an order of magnitude higher than its values at 30 torr. Clearly, the reduction of pressure strongly favors the production of 1-methylene-2-indanyl **p4**, which is a critical precursor of benzofulvene (**p1**)/naphthalene (**p0**) at high temperatures. Even though the yield of the endoergic **p6** and **p7** products exceeds that of **p4** above 1400 K, the benzyl plus propargyl rate constant to **p4** plus atomic hydrogen does not fall below $10^{-14}$ cm$^3$ molecule$^{-1}$ s$^{-1}$ up to 2000 K. Thus, the reaction mechanism is applicable to the conditions of circumstellar envelopes of carbon rich stars with lower pressures stimulating the higher yield of the $C_{10}H_8$ isomers. In contrast, the benzyl–propargyl reaction is predicted

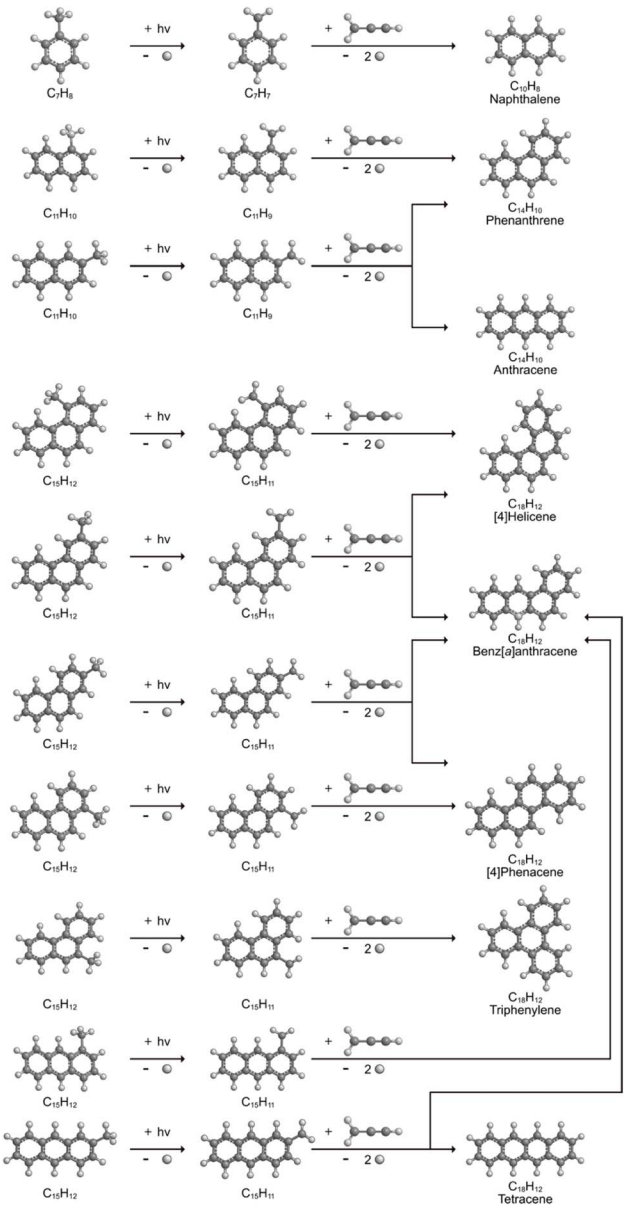


Fig. 6 Selected PAHs carrying a benzyl moiety in conjunction with a non-substituted carbon atom at the *ortho* position of the methylene group ($-CH_2^{\bullet}$) can undergo overall ring annulation upon multi step reactions with the propargyl radical.

not to be a viable source of naphthalene in low-temperature conditions such as in cold molecular clouds like the Taurus Molecular Cloud 1 (TMC-1). The rate constants computed in the 70–200 K range are illustrated in Fig. S5 (ESI).† While the total rate constant rises above $10^{-10}$ cm$^3$ molecule$^{-1}$ s$^{-1}$ at low temperatures, the reaction nearly exclusively forms $C_{10}H_{10}$ (**i1**) *via* radiative stabilization. A small fraction of **p4** is produced with the rate constant on the order of $10^{-14}$ cm$^3$ molecule$^{-1}$ s$^{-1}$, however, at such low temperatures, the 1-methylene-2-indanyl radical (**p4**) does not possess sufficient energy to decompose *via* atomic hydrogen loss. The rate constants for the production of benzofulvene (**p1**) and naphthalene (**p0**) along with molecular hydrogen in the primary reaction are evaluated to be as low as $10^{-17}$ and $\sim 10^{-19}$ cm$^3$ molecule$^{-1}$ s$^{-1}$, respectively, and hence can be neglected. Therefore, despite being classified as a radical–radical reaction, bimolecular reactions between the propargyl and the benzyl radicals are closed in cold molecular clouds, and radiative stabilization of the initial collision complex may control the outcome of the reaction, whereas in circumstellar envelopes, naphthalene (**p0**) along with minor fractions of benzofulvene (**p1**) can be formed *via* a complex sequence of chemical reactions (1) to (4).

## Conclusion & outlook

The radical–radical reaction of propargyl with benzyl represents a fundamental benchmark of a benzannulation of an aromatic ring and could imply a versatile multistep mechanism of PAH growth in high temperature circumstellar envelopes of carbon rich stars and planetary nebulae as their descendants. Each PAH carrying a benzyl moiety in conjunction with a non-substituted carbon atom at the *ortho* position of the methylene group ($-\dot{C}H_2$) may undergo ring annulation upon reaction with the propargyl radical (Fig. 6). In strong analogy of the benzyl–propargyl system leading *via* benzannulation through hydrogen assisted isomerization to the simplest PAH carrying two six-membered rings, *i.e.* naphthalene ($C_{10}H_8$), reactions of 1′- and 2′-methylnaphthyl ($C_{10}H_7\dot{C}H_2$) with propargyl may eventually access anthracene and phenanthrene ($C_{14}H_{10}$), which carry three six-membered rings. In deep space, 1′- and 2′-methylnaphthyl ($C_{10}H_7\dot{C}H_2$) can be generated easily *via* photodissociation of 1- and 2-methylnaphthalene ($C_{10}H_7CH_3$), respectively, which in turn can be formed *via* the barrierless reactions of tolyl radicals ($C_6H_4\cdot CH_3$) with vinylacetylene ($C_4H_4$) as demonstrated recently in crossed molecular beams experiments.[46,47] Further molecular mass growth processes commence with the photolysis and carbon–hydrogen bond cleavage within the methyl group of distinct isomers of methylated phenanthrenes and anthracenes; upon reaction with the propargyl radicals and eventual molecular hydrogen loss, five distinct $C_{18}H_{12}$ isomers including the simplest representatives of helicenes ([4]helicene), acenes (tetracene), and phenacenes ([4]phenacene) can be synthesized in deep space *via* entrance-barrierless, exoergic bimolecular reactions involving the propargyl radical (Fig. 5). Therefore, this novel reaction mechanism, which we designate Propargyl Addition–BenzAnnulation (PABA), may represent a critical sink of interstellar propargyl radicals as detected at substantial fractional abundance relative to molecular hydrogen of $8.7 \times 10^{-9}$ toward TMC-1;[35] this complex reaction sequence may represent a unusual molecular mass growth process potentially rivaling the Hydrogen Abstraction–Acetylene Addition (HACA)[48–50] and Hydrogen Abstraction–Vinylacetylene Addition (HAVA) mechanisms.[40,51–54] Therefore, the conceptual framework of the Propargyl Addition–BenzAnnulation (PABA) mechanism involving the reaction of astronomically abundant propargyl radicals with aromatic radicals carrying the radical center at the off-ring methylene moiety (aromatic$\dot{C}H_2$) provides a promising source of polyaromatics in carbon-rich, high temperature circumstellar environments thus bringing us closer to the unraveling of the aromatic nature of the universe we live in.

## Data availability

Essential data are provided in the main text and the ESI.† Additional data can be available from the corresponding author upon reasonable request.

## Author contributions

R. I. K. designed the experiment; C. H., and W. L. carried out the experimental measurements; M. A. supervised the experiment; C. H. performed the data analysis; V. S. K., P. S. P., M. V. Z., V. N. A., A. N. M., and A. M. M. carried out the theoretical analysis; R. I. K., A. M. M., and M. A. discussed the data; C. H., R. I. K., A. M. M., and M. A. wrote the paper.

## Conflicts of interest

The authors declare no conflict of interest.

## Acknowledgements

This work was supported by the US Department of Energy, Basic Energy Sciences DE-FG02-03ER15411 (experimental studies) and DE-FG02-04ER15570 (computational studies) to the University of Hawaii (UH) and Florida International University (FIU), respectively. W. L. and M. A. were supported by the Director, Office of Science, Office of Basic Energy Sciences, of the U.S. Department of Energy under Contract No. DE-AC02-05CH11231, through the Gas Phase Chemical Physics program of the Chemical Sciences Division. The Advanced Light Source at Berkeley is also supported under Contract No. DE-AC02-05CH11231. *Ab initio* calculations at Samara were supported by the Ministry of Higher Education and Science of the Russian Federation under Grant No. 075-15-2021-597.

## References

1 P. Swings and L. Rosenfeld, Considerations Regarding Interstellar Molecules, *Astrophys. J.*, 1937, **86**, 483–486.
2 A. Leger and J. L. Puget, Identification of the "Unidentified" IR Emission Features of Interstellar Dust?, *Astron. Astrophys.*, 1984, **137**, L5–L8.

3 G. Nagendrappa, Benzene and Its Isomers, *Resonance*, 2001, **6**, 74–78.
4 T. C. Dinadayalane, U. D. Priyakumar and G. N. Sastry, Exploration of $C_6H_6$ Potential Energy Surface: A Computational Effort to Unravel the Relative Stabilities and Synthetic Feasibility of New Benzene Isomers, *J. Phys. Chem. A*, 2004, **108**, 11433–11448.
5 J. A. Miller and C. F. Melius, Kinetic and Thermodynamic Issues in the Formation of Aromatic Compounds in Flames of Aliphatic Fuels, *Combust. Flame*, 1992, **91**, 21–39.
6 C. F. Melius, J. A. Miller and E. M. Evleth, Unimolecular Reaction Mechanisms Involving $C_3H_4$, $C_4H_4$, and $C_6H_6$ Hydrocarbon Species, *Symp. (Int.) Combust.*, 1992, **24**, 621–628.
7 L. K. Madden, A. M. Mebel, M.-C. Lin and C. F. Melius, Theoretical Study of the Thermal Isomerization of Fulvene to Benzene, *J. Phys. Org. Chem.*, 1996, **9**, 801–810.
8 A. M. Mebel, S. H. Lin, X. M. Yang and Y. T. Lee, Theoretical Study on the Mechanism of the Dissociation of Benzene. The $C_5H_3$ + $CH_3$ Product Channel, *J. Phys. Chem. A*, 1997, **101**, 6781–6789.
9 A. M. Mebel, M.-C. Lin, D. Chakraborty, J. Park, S. H. Lin and Y. T. Lee, Ab Initio Molecular Orbital/Rice–Ramsperger–Kassel–Marcus Theory Study of Multichannel Rate Constants for the Unimolecular Decomposition of Benzene and the H + $C_6H_5$ Reaction Over the Ground Electronic State, *J. Chem. Phys.*, 2001, **114**, 8421–8435.
10 V. V. Kislov, T. L. Nguyen, A. M. Mebel, S. H. Lin and S. C. Smith, Photodissociation of Benzene under Collision-Free Conditions: An Ab Initio/Rice–Ramsperger–Kassel–Marcus Study, *J. Chem. Phys.*, 2004, **120**, 7008–7017.
11 J. A. Miller and S. J. Klippenstein, The Recombination of Propargyl Radicals: Solving the Master Equation, *J. Phys. Chem. A*, 2001, **105**, 7254–7266.
12 J. A. Miller and S. J. Klippenstein, The Recombination of Propargyl Radicals and Other Reactions on a $C_6H_6$ Potential, *J. Phys. Chem. A*, 2003, **107**, 7783–7799.
13 M. Frenklach and E. D. Feigelson, Formation of Polycyclic Aromatic Hydrocarbons in Circumstellar Envelopes, *Astrophys. J.*, 1989, **341**, 372–384.
14 R. Zenobi, J.-M. Philippoz, R. N. Zare, M. R. Wing, J. L. Bada and K. Marti, Organic Compounds in the Forest Vale, H4 Ordinary Chondrite, *Geochim. Cosmochim. Acta*, 1992, **56**, 2899–2905.
15 Y. M. Rhee, T. J. Lee, M. S. Gudipati, L. J. Allamandola and M. Head-Gordon, Charged Polycyclic Aromatic Hydrocarbon Clusters and the Galactic Extended Red Emission, *Proc. Natl. Acad. Sci. U. S. A.*, 2007, **104**, 5274–5278.
16 A. G. G. M. Tielens, Interstellar Polycyclic Aromatic Hydrocarbon Molecules, *Annu. Rev. Astron. Astrophys.*, 2008, **46**, 289–337.
17 P. Ehrenfreund and M. A. Sephton, Carbon Molecules in Space: From Astrochemistry to Astrobiology, *Faraday Discuss.*, 2006, **133**, 277–288.
18 E. Herbst and E. F. Van Dishoeck, Complex Organic Interstellar Molecules, *Annu. Rev. Astron. Astrophys.*, 2009, **47**, 427–480.
19 J. L. Puget and A. Léger, A New Component of the Interstellar Matter: Small Grains and Large Aromatic Molecules, *Annu. Rev. Astron. Astrophys.*, 1989, **27**, 161–198.
20 P. Schmitt-Kopplin, Z. Gabelica, R. D. Gougeon, A. Fekete, B. Kanawati, M. Harir, I. Gebefuegi, G. Eckel and N. Hertkorn, High Molecular Diversity of Extraterrestrial Organic Matter in Murchison Meteorite Revealed 40 Years after Its Fall, *Proc. Natl. Acad. Sci. U. S. A.*, 2010, **107**, 2763–2768.
21 B. A. McGuire, R. A. Loomis, A. M. Burkhardt, K. L. K. Lee, C. N. Shingledecker, S. B. Charnley, I. R. Cooke, M. A. Cordiner, E. Herbst, S. Kalenskii, M. A. Siebert, E. R. Willis, C. Xue, A. J. Remijan and M. C. McCarthy, Detection of Two Interstellar Polycyclic Aromatic Hydrocarbons via Spectral Matched Filtering, *Science*, 2021, **371**, 1265–1269.
22 L. M. Ziurys, The Chemistry in Circumstellar Envelopes of Evolved Stars: Following the Origin of the Elements to the Origin of Life, *Proc. Natl. Acad. Sci. U. S. A.*, 2006, **103**, 12274–12279.
23 A. W. Jasper and N. Hansen, Hydrogen-assisted Isomerizations of Fulvene to Benzene and of Larger Cyclic Aromatic Hydrocarbons, *Proc. Combust. Inst.*, 2013, **34**, 279–287.
24 C. S. McEnally, L. D. Pfefferle, B. Atakan and K. Kohse-Höinghaus, Studies of Aromatic Hydrocarbon Formation Mechanisms in Flames: Progress towards Closing the Fuel Gap, *Prog. Energy Combust. Sci.*, 2006, **32**, 247–294.
25 H. Richter and J. B. Howard, Formation and Consumption of Single-ring Aromatic Hydrocarbons and their Precursors in Premixed Acetylene, Ethylene and Benzene Flames, *Phys. Chem. Chem. Phys.*, 2002, **4**, 2038–2055.
26 A. G. G. M. Tielens and L. J. Allamandola, in *Physics and Chemistry at Low Temperatures*, ed. L. Khriachtchev, Pan Stanford Publishing, Singapore, 2011.
27 K. Fujishima, S. Dziomba, H. Yano, S. I. Kebe, M. Guerrouache, B. Carbonnier and L. J. Rothschild, The Non-Destructive Separation of Diverse Astrobiologically Relevant Organic Molecules by Customizable Capillary Zone Electrophoresis and Monolithic Capillary Electrochromatography, *Int. J. Astrobiol.*, 2019, **18**, 562–574.
28 L. J. Allamandola, S. A. Sandford and B. Wopenka, Interstellar Polycyclic Aromatic Hydrocarbons and Carbon in Interplanetary Dust Particles and Meteorites, *Science*, 1987, **237**, 56–59.
29 A. G. G. M. Tielens, C. van Kerckhoven, E. Peeters and S. Hony, Astrochemistry: From Molecular Clouds to Planetary Systems, presented in part at the *Symposium - International Astronomical Union*, 2000, vol. 197.
30 I. Cherchneff, J. R. Barker and A. G. G. M. Tielens, Polycyclic Aromatic Hydrocarbon Formation in Carbon-Rich Stellar Envelopes, *Astrophys. J.*, 1992, **401**, 269–287.
31 M. Cohen, A. G. G. M. Tielens and J. D. Bregman, Mid-Infrared Spectra of WC 9 Stars: The Composition of Circumstellar and Interstellar Dust, *Astrophys. J.*, 1989, **344**, L13–L16.

32 E. R. Micelotta, A. P. Jones and A. G. G. M. Tielens, Polycyclic Aromatic Hydrocarbon Processing in Interstellar Shocks, *Astron. Astrophys.*, 2010, **510**, A36.
33 N. Hansen, B. Yang, M. Braun-Unkhoff, A. Ramirez and G. Kukkadapu, Molecular-growth Pathways in Premixed Flames of Benzene and Toluene Doped with Propyne, *Combust. Flame*, 2022, **243**, 112075.
34 A. Matsugi and A. Miyoshi, Computational Study on the Recombination Reaction between Benzyl and Propargyl Radicals, *Int. J. Chem. Kinet.*, 2012, **44**, 206–218.
35 M. Agúndez, C. Cabezas, B. Tercero, N. Marcelino, J. D. Gallego, P. de Vicente and J. Cernicharo, Discovery of the Propargyl Radical ($CH_2CCH$) in TMC-1: One of the Most Abundant Radicals Ever Found and a Key Species for Cyclization to Benzene in Cold Dark Clouds, *Astron. Astrophys.*, 2021, **647**, L10.
36 M. V. Zagidullin, R. I. Kaiser, D. P. Porfiriev, I. P. Zavershinskiy, M. Ahmed, V. N. Azyazov and A. M. Mebel, Functional Relationships between Kinetic, Flow, and Geometrical Parameters in a High-Temperature Chemical Microreactor, *J. Phys. Chem. A*, 2018, **122**, 8819–8827.
37 R. I. Kaiser, L. Zhao, W. Lu, M. Ahmed, V. S. Krasnoukhov, V. N. Azyazov and A. M. Mebel, Unconventional Excited-State Dynamics in the Concerted Benzyl ($C_7H_7$) Radical Self-Reaction to Anthracene ($C_{14}H_{10}$), *Nat. Commun.*, 2022, **13**, 786.
38 L. Zhao, W. Lu, M. Ahmed, M. V. Zagidullin, V. N. Azyazov, A. N. Morozov, A. M. Mebel and R. I. Kaiser, Gas-Phase Synthesis of Benzene via the Propargyl Radical Self-Reaction, *Sci. Adv.*, 2021, **7**, eabf0360.
39 F. Qi, Combustion Chemistry Probed by Synchrotron VUV Photoionization Mass Spectrometry, *Proc. Combust. Inst.*, 2013, **34**, 33–63.
40 L. Zhao, R. I. Kaiser, B. Xu, U. Ablikim, M. Ahmed, M. V. Zagidullin, V. N. Azyazov, A. H. Howlader, S. F. Wnuk and A. M. Mebel, VUV Photoionization Study of the Formation of the Simplest Polycyclic Aromatic Hydrocarbon: Naphthalene ($C_{10}H_8$), *J. Phys. Chem. Lett.*, 2018, **9**, 2620–2626.
41 Y. Li, J. Yang and Z. Cheng, *Photoionization Cross Section Database (Version 2.0)*, National Synchrotron Radiation Laboratory, Hefei, China, 2017, **http://flame.nsrl.ustc.edu.cn/database/data.php**.
42 V. S. Krasnoukhov, P. S. Pivovarov, M. V. Zagidullin, V. N. Azyazov, A. M. Mebel and A. N. Morozov, Formation of Two-ring Polycyclic Aromatic Hydrocarbons via the Recombination of Benzyl and Propargyl Radicals under the Circumstellar Envelopes Conditions of Asymptotic Giant Branch Stars, *Astron. Rep.*, 2022, **66**, 811–826.
43 D. W. Kohn, H. Clauberg and P. Chen, Flash Pyrolysis Nozzle for Generation of Radicals in a Supersonic Jet Expansion, *Rev. Sci. Instrum.*, 1992, **63**, 4003–4005.
44 *NIST Chemistry WebBook, SRD 69*, **https://webbook.nist.gov/chemistry/**.
45 A. M. Mebel, Y. Georgievskii, A. W. Jasper and S. J. Klippenstein, Pressure-Dependent Rate Constants for PAH Growth: Formation of Indene and Its Conversion to Naphthalene, *Faraday Discuss.*, 2016, **195**, 637–670.
46 D. S. N. Parker, B. B. Dangi, R. I. Kaiser, A. Jamal, M. N. Ryazantsev, K. Morokuma, A. Korte and W. Sander, An Experimental and Theoretical Study on the Formation of 2-Methylnaphthalene ($C_{11}H_{10}/C_{11}H_3D_7$) in the Reactions of the Para-Tolyl ($C_7H_7$) and Para-Tolyl-d7 ($C_7D_7$) with Vinylacetylene ($C_4H_4$), *J. Phys. Chem. A*, 2014, **118**, 2709–2718.
47 T. Yang, L. Muzangwa, R. I. Kaiser, A. Jamal and K. Morokuma, A Combined Crossed Molecular Beam and Theoretical Investigation of the Reaction of the Meta-Tolyl Radical with Vinylacetylene–toward the Formation of Methylnaphthalenes, *Phys. Chem. Chem. Phys.*, 2015, **17**, 21564–21575.
48 M. Frenklach, D. W. Clary, W. C. Gardiner Jr and S. E. Stein, Detailed Kinetic Modeling of Soot Formation in Shock-Tube Pyrolysis of Acetylene, *Symp. (Int.) Combust.*, 1985, **20**, 887–901.
49 M. Frenklach, Reaction Mechanism of Soot Formation in Flames, *Phys. Chem. Chem. Phys.*, 2002, **4**, 2028–2037.
50 M. Frenklach, On the Driving Force of PAH Production, *Symp. (Int.) Combust.*, 1989, **22**, 1075–1082.
51 R. I. Kaiser, L. Zhao, W. Lu, M. Ahmed, M. M. Evseev, V. N. Azyazov, A. M. Mebel, R. K. Mohamed, F. R. Fischer and X. Li, Gas-Phase Synthesis of Racemic Helicenes and Their Potential Role in the Enantiomeric Enrichment of Sugars and Amino Acids in Meteorites, *Phys. Chem. Chem. Phys.*, 2022, **24**, 25077–25087.
52 R. I. Kaiser and N. Hansen, An Aromatic Universe–A Physical Chemistry Perspective, *J. Phys. Chem. A*, 2021, **125**, 3826–3840.
53 R. I. Kaiser, D. S. N. Parker and A. M. Mebel, Reaction Dynamics in Astrochemistry: Low-Temperature Pathways to Polycyclic Aromatic Hydrocarbons in the Interstellar Medium, *Annu. Rev. Phys. Chem.*, 2015, **66**, 43–67.
54 A. M. Mebel and R. I. Kaiser, Formation of Resonantly Stabilised Free Radicals via the Reactions of Atomic Carbon, Dicarbon, and Tricarbon with Unsaturated Hydrocarbons: Theory and Crossed Molecular Beams Experiments, *Int. Rev. Phys. Chem.*, 2015, **34**, 461–514.